Transient natural convection in stored granular media
Proceedings of European Congress of Chemical Engineering (ECCE-6)
Copenhagen, 16-20 September 2007

Transient natural convection in stored granular media

J.G. Avila-Acevedo, E. Tsotsas

Thermal Process Engineering, Otto-von-Guericke-University Magdeburg, Universitaetsplatz 2, D-39106 Magdeburg, Germany

Abstract

Transient natural convection taking place in an originally isothermal cylinder filled with a porous medium after sudden change of wall temperature is studied experimentally and computationally. A mathematical model is developed, and the parameters influencing natural convection are identified. Results from simulations are compared with experiments allowing for model validation.

Keywords: Transient heat transfer, natural convection, porous media, homogeneous model

1. Introduction

Storage is one of the fundamental stages in the production and handling of granular materials like cereals, sugar, salts, polymers, etc. Depending on the conditions of the materials at the beginning of storage (temperature, moisture content, etc.) and to ambient conditions an equilibrium state will be reached by means of heat and mass transfer, which can produce an undesired variation of product quality by moisture migration and even condensation (the so-called “silo rain”) [1,2]. Because of the problems emerging during the storage of porous materials, it is important to understand the transport phenomena implied and realize, which factors have an influence, in order to control such undesirable effects. Before considering moisture migration, the problem of free convection must be analyzed and understood.

Most of the studies on heat transfer in porous media are related to horizontal or vertical steady state heat transfer (or the analogous mass transfer) applied to insulation, aquifers and nuclear reactors [3,4]. The study of transient heat transfer in stored porous media has been addressed mainly in agronomic engineering due to the important role played by such phenomena for grain preservation. Mathematical models for the prediction of temperature of silos have been previously developed for one, two and three-dimensional cylindrical configurations [5,6]. These works are highly focused on determining temperature distribution for different boundary

conditions (i.e. wall materials, solar radiation, wind, etc.), and some of them assume a negligible effect of natural convection within the medium based only on empirical observations (see among others [7]). In general, transient heat transfer in confined porous media has not been yet properly studied, although its importance is recognized in literature.

In this paper the effect of natural convection on transient heat transfer in porous media stored in a cylinder cooled at the exterior wall is mathematically and experimentally studied. A homogeneous model is derived considering local thermal equilibrium between the phases and taking the Darcy law as valid. Having analyzed the equations, the most important parameters influencing the transient heat transfer process are identified. Experiments are performed in a laboratory scale silo showing the transient behaviour of temperature as a function of the parameters. The experimental results are compared with the simulations allowing for model validation.

2. Mathematical problem

2.1 *System considered*

The system under analysis is a cylindrical silo with radius R and height H that is completely filled with a porous medium (Fig. 1). Axial symmetry is assumed and the silo is considered as thermally insulated at top and bottom. The porous medium has initially an uniform temperature of T_0. A transient cooling process takes place because the wall temperature is assumed to have a constant and lower value of T_W. Under these conditions heat transfer may be accompanied by convection due to buoyant forces. The aim is to determine the influence of natural convection on the cooling process.

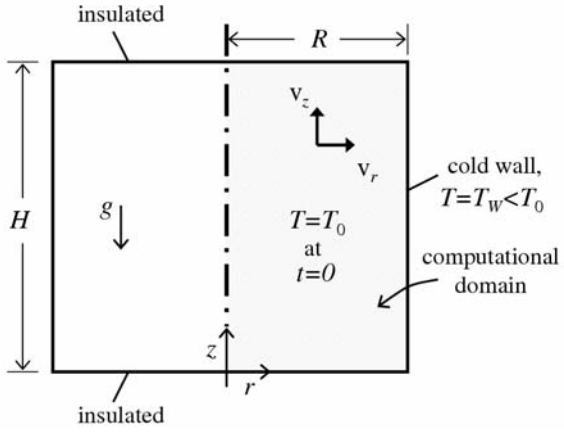

Fig. 1. Scheme of cylindrical silo and computational domain.

2.2 *Basic equations*

A model for transient heat transfer in a fluid-saturated porous medium is proposed following [8,9,10]. We assume an isotropic porous medium, thermal equilibrium between phases, negligible heat generation due to the flow and validity of Darcy's law. Considering the following scales:

$$\hat{r} = \frac{r}{R},\ \hat{z} = \frac{z}{H},\ \theta = \frac{T - T_W}{T_0 - T_W}, \tag{1,2,3}$$

$$\hat{\mathrm{v}}_z = \frac{\mathrm{v}_z}{U_0},\ \ \hat{\mathrm{v}}_r = \frac{H}{R}\frac{\mathrm{v}_r}{U_0},\ \ \tau = \frac{\alpha^* t}{\sigma_b R^2}, \tag{4,5,6}$$

the equations expressing the conservation of mass, momentum and energy are obtained in the dimensionless form

$$\frac{1}{\hat{r}}\frac{\partial}{\partial \hat{r}}\left(\hat{r}\ \hat{\mathrm{v}}_r\right) + \frac{\partial}{\partial \hat{z}}\left(\hat{\mathrm{v}}_z\right) = 0, \tag{7}$$

$$\left(\frac{R}{H}\right)^2 \frac{\partial \hat{\mathrm{v}}_r}{\partial \hat{z}} - \frac{\partial \hat{\mathrm{v}}_z}{\partial \hat{r}} = -\frac{\partial \theta}{\partial \hat{r}}, \tag{8}$$

$$\frac{\partial \theta}{\partial \tau} + \mathrm{Ra}_b\left(\frac{R}{H}\right)^2\left[\hat{\mathrm{v}}_r \frac{\partial \theta}{\partial \hat{r}} + \hat{\mathrm{v}}_z \frac{\partial \theta}{\partial \hat{z}}\right] = \frac{1}{\hat{r}}\frac{\partial}{\partial \hat{r}}\left(\hat{r}\frac{\partial \theta}{\partial \hat{r}}\right) + \left(\frac{R}{H}\right)^2 \frac{\partial^2 \theta}{\partial \hat{z}^2}, \tag{9}$$

with the boundary conditions at horizontal walls:

$$\hat{z} = 0,\ \hat{z} = 1: \quad \frac{\partial \theta}{\partial \hat{z}} = 0,\ \hat{\mathrm{v}}_z = 0,\ \hat{\mathrm{v}}_r = \text{free}, \tag{10a}$$

at vertical walls:

$$\hat{r} = 0: \quad \frac{\partial \theta}{\partial \hat{r}} = 0,\ \hat{\mathrm{v}}_r = 0,\ \hat{\mathrm{v}}_z \ \text{free}, \tag{10b}$$

$$\hat{r} = 1: \quad \theta = 0,\ \hat{\mathrm{v}}_r = 0,\ \hat{\mathrm{v}}_z \ \text{free}, \tag{10c}$$

and the initial conditions:

$$\tau = 0: \quad \theta = 1,\ \hat{\mathrm{v}}_r = 0,\ \hat{\mathrm{v}}_z = 0. \tag{11}$$

The most relevant parameters appearing are the aspect ratio of the cylinder (R/H) and the modified porous media Rayleigh number

$$\mathrm{Ra}_\mathrm{b} = \frac{Kg\rho_{f,0}\beta H}{\mu\alpha^*}(T_0 - T_W). \tag{12}$$

The latter depends on temperature difference, fluid properties (density ρ_f, viscosity μ, coefficient of thermal expansion β), bed properties (bed permeability K, fluid based bed thermal diffusivity α^*), and silo height H.

Eq.(8) is a combined flow expression obtained by cross differentiation of Darcy flow in radial and axial directions. Following Bejan [10], the Boussinesq approximation

$$\rho_f = \rho_{f,0}\left[1 - \beta\left(T - T_0\right)\right] \tag{13}$$

has been used to avoid pressure calculations. The bed capacity ratio σ_b and the quantity α^* appearing in Eq. (6) are described by the relationships

$$\sigma_b = \frac{(1-\psi)\rho_s c_s + \psi\rho_f c_{P,f}}{\rho_f c_{P,f}} = \frac{\rho_b c_b}{\rho_f c_{P,f}} \tag{14}$$

and

$$\alpha^* = \frac{\lambda_b}{\rho_f c_{P,f}} = \frac{\lambda_b}{\rho_b c_b} \frac{\rho_b c_b}{\rho_f c_{P,f}} = \alpha_b \sigma_b , \tag{15}$$

where α_b is the porous medium thermal diffusivity. The permeability is related to bed particle diameter *d* using the Carman-Kozeny equation [11]

$$K = \frac{d^2 \psi^3}{150(1-\psi)^2} , \tag{16}$$

where ψ is the bed porosity. The variable U_0 appearing in Eqs. (4) and (5) is the maximal velocity of the fluid attainable for a specific porous medium and temperature difference [12] and can be expressed as

$$U_0 = \frac{K g_z \rho_{f,0} \beta}{\mu} (T_0 - T_W) . \tag{17}$$

3. Numerical solution

3.1 *Equations*

Before solving the system of equations represented by Eqs. (7) to (11), it is convenient to simplify the problem. Following [13], a stream function is defined as

$$\hat{v}_r = \frac{1}{\hat{r}} \frac{\partial \chi}{\partial \hat{z}} , \qquad \hat{v}_z = -\frac{1}{\hat{r}} \frac{\partial \chi}{\partial \hat{r}} . \tag{18a,b}$$

It is easy to observe that these equations satisfy continuity. The system of equations is reduced to only two partial differential equations for potential flow and for energy

$$\left(\frac{R}{H}\right)^2 \frac{\partial^2 \chi}{\partial \hat{z}^2} + \frac{\partial^2 \chi}{\partial \hat{r}^2} - \frac{1}{\hat{r}} \frac{\partial \chi}{\partial \hat{r}} = -\hat{r} \frac{\partial \theta}{\partial \hat{r}} , \tag{19}$$

$$\frac{\partial \theta}{\partial \tau} + \mathrm{Ra}_b \left(\frac{R}{H}\right)^2 \left[\frac{1}{\hat{r}} \frac{\partial \chi}{\partial \hat{z}} \frac{\partial \theta}{\partial \hat{r}} - \frac{1}{\hat{r}} \frac{\partial \chi}{\partial \hat{r}} \frac{\partial \theta}{\partial \hat{z}}\right] = \frac{1}{\hat{r}} \frac{\partial}{\partial \hat{r}} \left(\hat{r} \frac{\partial \theta}{\partial \hat{r}}\right) + \left(\frac{R}{H}\right)^2 \frac{\partial^2 \theta}{\partial \hat{z}^2} , \tag{20}$$

with the boundary conditions at horizontal walls

$$\hat{z} = 0 : \ \chi = 0 , \ \frac{\partial \theta}{\partial \hat{z}} = 0 , \quad \hat{z} = 1 : \ \chi = 0 , \ \frac{\partial \theta}{\partial \hat{z}} = 0 ; \tag{21a}$$

at vertical walls

$$\hat{r} = 0 : \ \chi = 0 , \ \frac{\partial \theta}{\partial \hat{r}} = 0 \ \text{(symmetry)}, \quad \hat{r} = 1 : \ \chi = 0 , \ \theta = 0 ; \tag{21b}$$

and the initial conditions

$$\tau = 0 : \ \chi = 0 , \ \theta = 1 . \tag{22}$$

The system of Eqs. (19) to (22) can be solved for θ and χ using a proper numerical method.

3.2 *Numerical method*

A finite differences method with central differencing scheme is used for the numerical solution of the problem, including a line-by-line tridiagonal matrix algorithm (TDMA) method for solving the set of algebraic equations obtained after discretizing the potential flow equation, and a Jacobi method for solving the set of algebraic equations after discretizing the energy equation [14,15]. For given initial conditions, the set of discretized energy equations is solved by marching explicitly in time with a small time step, obtaining an initial temperature field. Then, the set of discretized potential flow equations is solved for the temperature field, obtaining the velocity field for the next time step. Afterwards, the temperature field is calculated for the next time step, but now considering the velocity field, closing the loop. This loop is followed until a defined time has been reached.

To ensure accuracy and numerical stability, proper spatial and temporal grids must be used. The order of error with the used discretization is $O(\Delta r)^2$, $O(\Delta z)^2$ in space and $O(\Delta\tau)$ in time. Grid independence was checked using grids of different sizes. For this study a grid of 80x80 lines was chosen. The number of time iterations selected was over 60,000, depending on the values of the parameters.

3.3 *Program verification*

For program verification, Eq. (20) is simplified by neglecting the convective terms (that means by assuming Ra_b=0) and transforming it into a 1D problem for $(R/H)^2$<<1, which is the case of an infinite cylinder. We obtain

$$\frac{\partial\theta}{\partial\tau} = \frac{1}{\hat{r}}\frac{\partial}{\partial\hat{r}}\left(\hat{r}\frac{\partial\theta}{\partial\hat{r}}\right) \tag{23}$$

with the boundary and initial conditions

$$\hat{r}=0:\ \frac{\partial\theta}{\partial\hat{r}}=0,\quad \hat{r}=1:\ \theta=0,\quad \tau=0:\ \theta=0. \tag{24}$$

This equation describes one dimensional transient heat transfer in an infinite cylinder. According to [16], the solution has the form

$$\theta(\hat{r},\tau) = 2\sum_{n=1}^{\infty}\frac{J_0(\hat{r}\lambda_n)}{\lambda_n J_1(\lambda_n)}\exp\left(-\lambda_n{}^2\tau\right), \tag{25a}$$

where the characteristic values λ_n are the roots of the equation

$$J_0(\lambda_n)=0, \tag{25b}$$

and J_0 and J_1 are the zeroth- and first-order Bessel functions of the first kind, respectively.

In Fig. 2, calculated dimensionless temperatures are plotted against radial position for different dimensionless times and compared against analytical values obtained from Eq. (25). Both results are practically indistinguishable, with an error of less than

0.2%. A comparison between simulated and experimental bed center temperature is shown in Fig 3, observing a good agreement. For the specific experimental conditions, natural convection can be neglected, see Table 1.

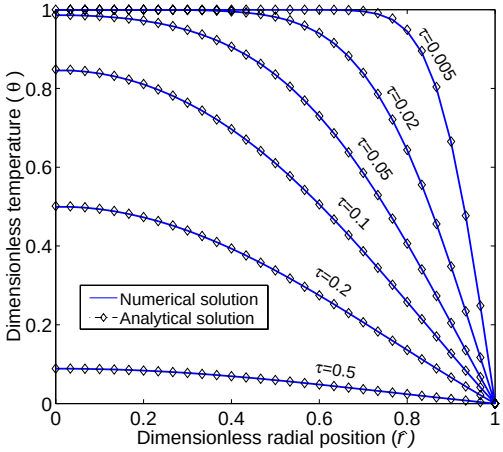

Fig. 2. Comparison between numerical and analytical solution for only conduction case.

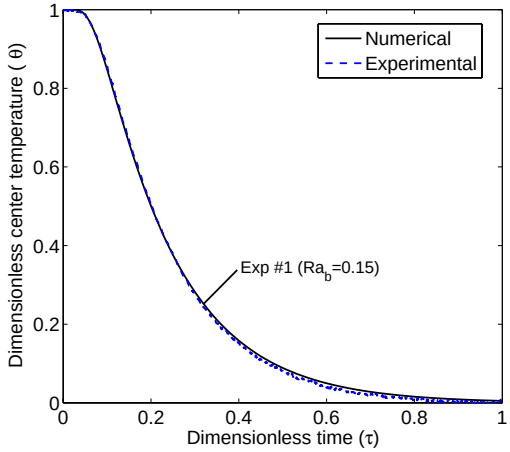

Fig. 3. Comparison between numerical and experimental results for only conduction case.

4. Experimental setup

The experimental apparatus was a laboratory scale silo, consisting of a jacketed copper cylinder of internal radius 19.5 mm and height 265 mm insulated at top and bottom, as it is schematically represented in Fig. 4. The cylinder was heated up and cooled down by water loops flowing through the jacket. Thermocouples placed in the center of the cylinder and at jacket inlet and outlet were used for monitoring bed temperature as well as fluid temperature. The particulate material consisted of commercially available glass beads with mean diameter 1.82 and 3.35 mm. The packed height (H) can be modified by placing additional insulation to the lids of the cylinder.

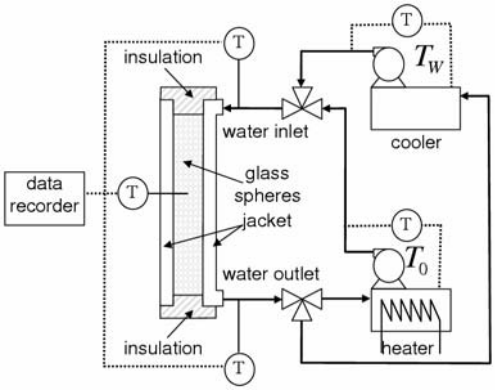

Fig. 4. Experimental setup.

For the experiments, bed temperature was set to an initial value with the help of the water loop. Then wall temperature was suddenly switched to a lower value. During the cooling process, temperatures were recorded until attainment of thermal equilibrium.

Beds of particles-air and particles-water were used to fill the cylinder. The former are only considered for determining glass thermal conductivity, based on the fact that when air is used at laboratory scale, natural convection is negligible because of the cylinder dimensions. As it can be observed in Table 1, values of Ra_b for the glass-air bed are small, and no natural convection effect is expected. This is indeed experimentally observed; all experimental lines measured with air are indistinguishable.

The particles-water bed is now used to investigate natural convection; different natural convection intensities, related to different values of Ra_b, were accomplished by variation of temperature difference, particle size and aspect ratio, as it is summarized in Table 1. By replacing the air with water a strong influence similar to that taking place in large, industrial silos is achieved and, therefore, a system for comfortably imitating free convection in industrial equipment at laboratory scale is obtained. This is demonstrated by the values of Ra_b, which make clear that natural convection intensity is strongly modified.

Table 1.
Experimental parameters.

Experiment	Fluid	d [mm]	ΔT [K]	H [mm]	R/H [-]	Ra_b [-]
1	air	3.35	5	152	0.128	0.15
2	water	3.35	20	152	0.128	682
3	water	3.35	50	152	0.128	1716
4	water	1.82	50	152	0.128	508
5	water	3.35	50	101	0.193	1137
6	water	3.35	30	101	0.193	682

4.1 *Bed thermal conductivity*

A fundamental parameter for describing heat transfer in beds is the bed thermal conductivity, λ_b. This property depends mainly on bed porosity (ψ), and on fluid and particle thermal conductivities (λ_f, λ_P). Although glass thermal conductivity is reported in literature, its value varies within a wide range, depending principally on glass components. To obtain an accurate value, the following procedure was followed.

Firstly, the bed thermal conductivity of air-glass bed is determined by fitting experimental results to the analytical solution of only conduction in an infinite cylinder, knowing that in such a case natural convection can be neglected [17]. Then, using the experimental value for the glass-air bed for a given air thermal conductivity ($\lambda_f = \lambda_{f,air}$) and ψ, glass thermal conductivity λ_P is obtained from the following equations of Zehner and Bauer [18]:

$$k_b = 1-\sqrt{1-\psi}+\sqrt{1-\psi}\,k_c\,, \tag{26a}$$

$$k_c = \frac{2}{N}\left(\frac{B}{N^2}\frac{k_P-1}{k_P}\ln\frac{k_P}{B}-\frac{B+1}{2}-\frac{B-1}{N}\right), \tag{26b}$$

$$B = 1.25\left(\frac{1-\psi}{\psi}\right)^{10/9},\ N = 1-\frac{B}{k_P} \tag{26c}$$

where

$$k_b = \frac{\lambda_b}{\lambda_f},\qquad k_c = \frac{\lambda_c}{\lambda_f},\qquad k_P = \frac{\lambda_P}{\lambda_f}. \tag{27}$$

Afterwards, the interstitial fluid (air) is replaced by water and the same equations are applied for known ψ , the obtained λ_P, and water thermal conductivity ($\lambda_f=\lambda_{f,water}$). In this way, the bed thermal conductivity for the case of a water-glass bed is obtained. This procedure is carried out for both particle sizes.

5. Results and discussion

As discussed previously, when the interstitial fluid is air, low values of the Rayleigh number are obtained and conduction heat transfer prevails. This situation corresponds to experiment 1 already shown in Fig 3, where a comparison of the simulated and experimental is also presented. The full description of simulation results corresponding to only conduction (Ra_b = 0) at different dimensionless times is shown in Fig. 5.

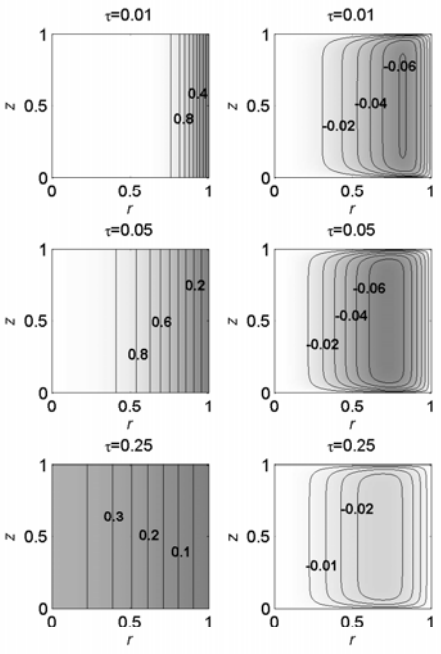

Fig. 5. Transient temperature profile and stream function for Ra_b =0.

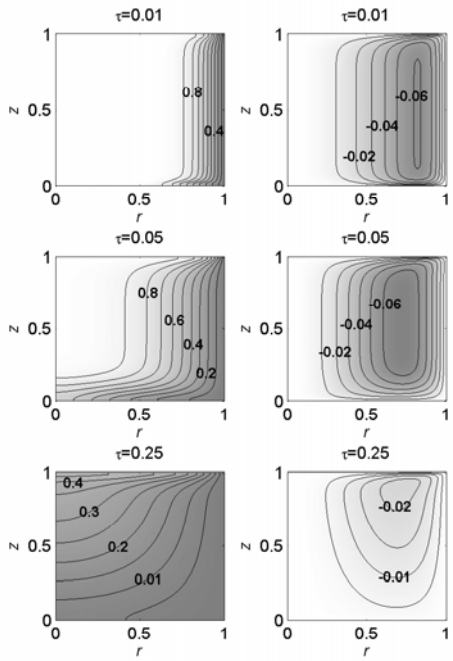

Fig. 6. Transient temperature profile and stream function, Ra_b =682, $R/H = 0.128$.

In this figure temperature profiles as well as the stream function obtained from simulations are depicted. It can be observed how the temperature decreases in radial direction forming straight isotherms that are characteristic for one dimensional heat transfer. This particular simulation is further used as a reference. It is worth to note that as soon as a temperature gradient appears, the potential of fluid movement could be also present, but because real velocities are obtained using Eqs. (4) and (5), they become zero. Thus, no movement of fluid exists.

The effect of natural convection is considerable as soon as the Rayleigh number increases. In Fig. 6, simulation results corresponding to experiment 2 are presented. Opposite to the conduction case, the isotherms are not longer straight and vertical. The fluid carries heat towards the upper part of the non-insulated wall, therefore a lower temperature is observed in the lower part of the bed. In Fig. 7a experimental and numerical results for different Rayleigh numbers corresponding to experiments 2 and 3 are presented. Higher values of Rayleigh number are obtained by increasing the temperature difference and, thus, the cooling rate.

When particle size is changed, as in experiment 4 in Fig. 7b, a similar effect to that of changing temperature difference is observed. This effect can be explained by observing that the Rayleigh number depends on bed permeability, as described in Eq. (12), and the former has the particle diameter as a parameter. Therefore, the larger the particle diameter the larger is the bed permeability. Because flow intensity is directly correlated to bed permeability, a stronger convective heat transport within the cylinder is expected for larger particles.

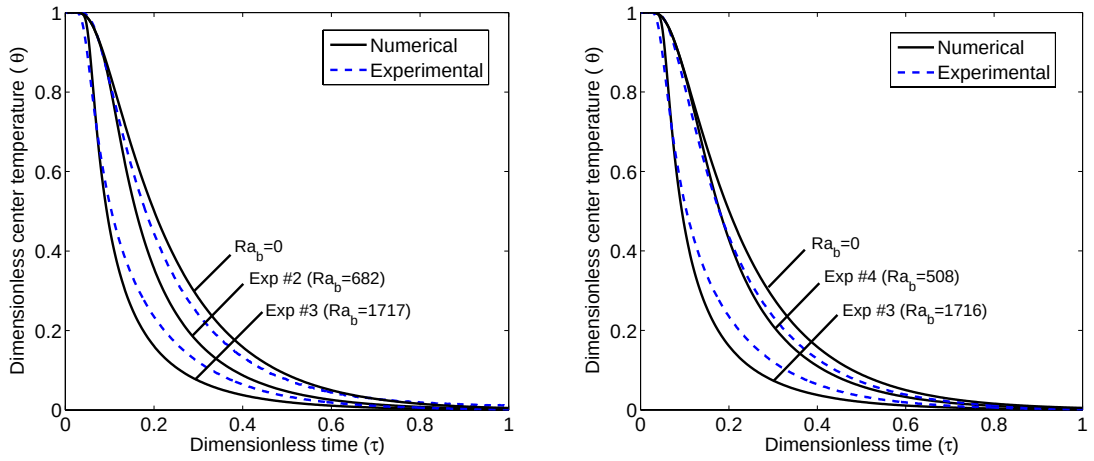

a) Effect of temperature difference. b) Effect of particle size.

Fig. 7. Comparison of simulated temperature with the temperature transient experimentally observed in the center of glass-water beds.

The effect of silo height is illustrated in Fig. 8a, where the cooling of a short bed (experiment 5) is compared with the cooling of a tall bed (experiment 3). One would expect faster cooling kinetics for experiment 3 because of the higher Rayleigh

number. However, exactly the opposite happens, indicating that the convective effect is larger for the short cylinder (experiment 5). This observation suggests that a second parameter is influencing natural convection.

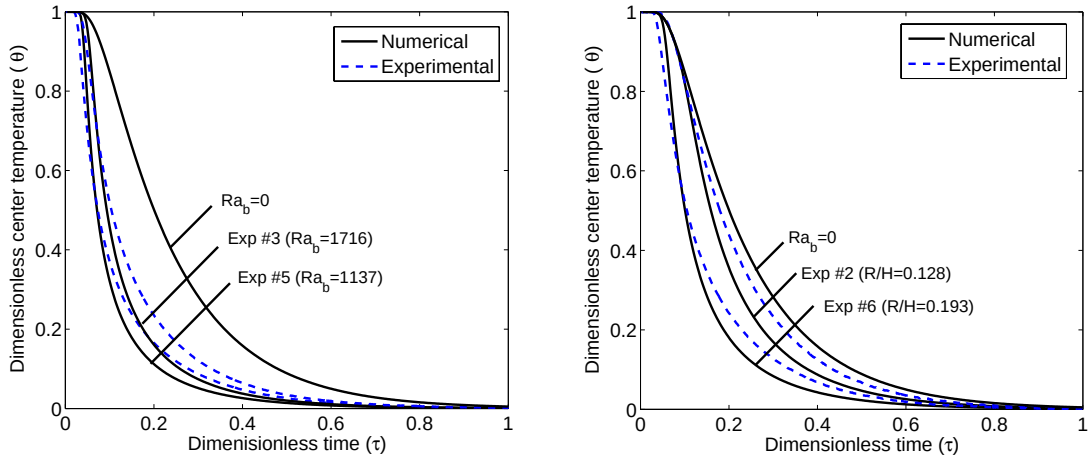

a) Effect of silo height. b) Effect of aspect ratio, Ra_b =682.

Fig. 8. Comparison of simulated with the experimentally observed temperatures in the center of glass-water beds.

When the silo height is changed keeping constant the Rayleigh number, the effect of the aspect ratio emerges. This influence can be explained by analysing Eqs. (8) and (9). On the one hand, the aspect ratio affects conduction by stretching the temperature profile. On the other hand, it assumes a similar role as the Rayleigh number, modifying the convective term so that for small values (that is, tall cylinders), natural convection may vanish even at relative large Rayleigh numbers. This situation is presented in Fig. 8b, where for a short cylinder (experiment 6) the center temperature decreases faster than for a tall cylinder (experiment 2), although the Rayleigh number is the same in both cases (Ra_b =682).

The effect of the parameters discussed above on the cooling process can be conveniently quantified by time constants for the attainment of thermal equilibrium, τ^*. These time constants are defined as the time lapsed before reaching 95% of the temperature step. When plotted as functions of the Rayleigh number and the aspect ratio, a parametric diagram as presented in Fig. 9 is obtained. From this diagram, criteria for neglecting the effect of natural convection on heat transfer may be established by observing the change of the time constants. In general, the effect of natural convection on heat transfer is small in the region under the curve corresponding to the value of τ^*=0.45.

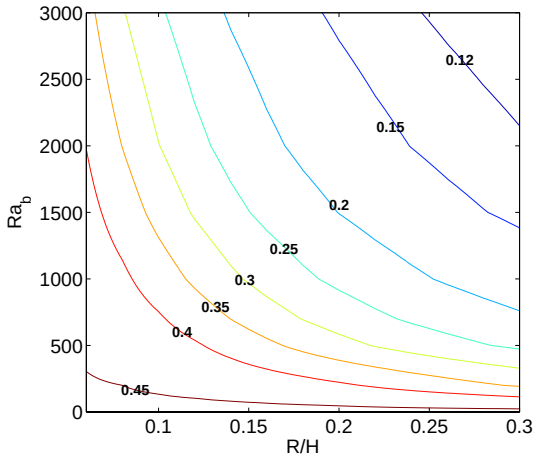

Fig. 9. Time constants for attainment of 95% of the temperature step at the center of the bed as functions of Ra_b and R/H .

6. Conclusions

The effect of natural convection on transient heat transfer taking place in a cylinder filled with a porous medium subject to sudden cooling has been investigated. After obtaining dimensionless expressions of the mathematical model, the porous media modified Rayleigh number and the aspect ratio are found to be the main parameters influencing natural convection. Natural convection has a very small influence on heat transfer in small cylinders filled with particles and air, as frequently used in the lab for the determination of packed bed thermal conductivity. However, it may have a strong influence in large, industrial silos. Considering the parameters mentioned above, a laboratory scale silo is obtained by exchanging the air with water. In this way, free convection in industrial equipment can be imitated. Additionally, the model has been validated by comparing simulations with experimental results. With the help of this model it is possible to simulate and study different cases of storage conditions, establishing criteria for identifying situations with a strong influence of natural convection in practice.

Acknowledgments

The financial support to the first author by the Deutscher Akademischer Austauschdienst (DAAD) and the Consejo Nacional de Ciencia y Tecnología (CONACyT) México is gratefully acknowledged.

Nomenclature

B deformation factor in model of Zehner and Bauer
c specific heat capacity [J/kg K]
c_P specific heat capacity of gas at constant pressure [J/kg K]
d mean particle diameter [m]

g	gravity acceleration [m/s^2]
H	cylinder height [m]
$J_{0,1}$	zeroth- and first-order Bessel functions of the first kind
K	permeability [m^2]
k	reduced conductivity [-]
N	Parameter in model of Zehner and Bauer
r	radial coordinate [m]
R	cylinder radius [m]
Ra_b	porous media modified Rayleigh number, Eq. (12) [-]
t	time [s]
T	temperature [°C]
U_0	reference flow velocity [m/s]
v	superficial velocity [m/s]
z	axial coordinate [m]

Greek symbols

α_b	effective bed thermal diffusivity [m^2/s]
α^*	modified bed thermal diffusivity, Eq. (15) [m^2/s]
β	coefficient of thermal expansion [1/K]
ΔT	temperature difference [K]
θ	dimensionless temperature [-]
λ	thermal conductivity [W/m K]
λ_n	eigenvalues [-]
μ	viscosity [kg/m s]
ρ	density [kg/m^3]
σ_b	heat capacity ratio, Eq. (14) [-]
τ	dimensionless time [-]
τ^*	time constant [-]
χ	stream function [-]
ψ	porosity [-]

Indices

b	bed
c	core
f	fluid
r	radial
s	solid
W	wall
z	axial
0	initial, reference
ˆ	dimensionless

References

[1] A. Lacey, M.P. Søresen, Danisco: Temperature and moisture gradients in sugar silos, In 32nd European Study Group with industry. Final report. Technical University of Denmark. 1998, pp. 37-46.
[2] M. Schneider, E. Tsotsas, On the predictability of silo rain: Modeling moisture migration in beds of particulates after drying, Proceedings of the First Nordic Drying Conference, Trondheim, Norway, 2001, Paper No. 15.
[3] J. Bear, A. Verruijt, Modeling ground water flow and pollution, D. Reidel Publishing Co, Holland 1987.
[4] D.A. Nield, A. Bejan, Convection in porous media, second ed., Springer Verlag, New York, 1999.
[5] D.S. Jayas, N.D.G. White, W.E. Muir, Stored grain ecosystems, Marcel Dekker Inc., New York, 1995.
[6] M.E. Casada, J.H. Young, Model for heat and moisture transfer in arbitrarily shaped two-dimensional porous media, Transactions of the ASAE 37 (6) (1994) 1927-1938.
[7] K. Alagusundaram, D.S. Jayas, N.D.G. White, W.E. Muir, Finite difference model of three-dimensional heat transfer in grain bins, Canadian Agricultural Engineering 32 (1990) 315-321.
[8] L. Burmeister, Convective heat transfer, second ed., John Wiley & Sons, Inc. 1993.
[9] U. Hornung, Homogenization and porous media, Springler Verlag, New York 1997.
[10] A. Bejan, Convection Heat Transfer, second ed., Wiley, New York, 1995.
[11] E.-U. Schlünder, E. Tsotsas, Wärmeübertragung in Festbetten, durchmischten Schüttgütern und Wirbelschichten, Thieme Verlag, Stuttgart-New York, 1988.
[12] A. Nakayama, PC-aided numerical heat transfer and convective flow, CRC Press Inc., London, 1995.
[13] E. Holzbecher, Modeling density-driven flow in porous media, Springer Verlag, Berlin, 1998.
[14] M. N. Ozisik, Finite difference methods in heat transfer, CRC Press, Florida, 1994.
[15] K. Muralidhar, T. Sundararajan, Computational fluid flow and heat transfer, Narosa Publishing House, New Delhi, 1995.
[16] H.S. Carslaw, J.C. Jaeger, Conduction of heat in solids, second ed, Clarendon Press-Oxford, 1959.
[17] W. Kwapinski, E. Tsotsas, Characterization of particulate materials in respect to drying, Drying Technology 24 (2006) 1083-1092.
[18] E. Tsotsas, H. Martin, Thermal conductivity of packed beds: A review, Chemical Engineering and Processing 22 (1987) 19-37.